VTT PUBLICATIONS 279

Microstructural degradation in compound tubes

Jorma Salonen & Pertti Auerkari

VTT Manufacturing Technology

TECHNICAL RESEARCH CENTRE OF FINLAND
ESPOO 1996

ISBN 951-38-4937-6
ISSN 1235-0621

JULKAISIJA – UTGIVARE – PUBLISHER

Valtion teknillinen tutkimuskeskus (VTT), Vuorimiehentie 5, PL 2000, 02044 VTT
puh. vaihde (09) 4561, faksi (09) 456 4374

Statens tekniska forskningscentral (VTT), Bergsmansvägen 5, PB 2000, 02044 VTT
tel. växel (09) 4561, fax (09) 456 4374

Technical Research Centre of Finland (VTT), Vuorimiehentie 5, P.O.Box 2000, FIN–02044 VTT, Finland
phone internat. + 358 9 4561, fax + 358 9 456 4374

VTT Valmistustekniikka, Materiaalien valmistustekniikka, Metallimiehenkuja 2–6, PL 1703, 02044 VTT
puh. vaihde (09) 4561, faksi (09) 463 118
VTT Tillverkningsteknik, Materialteknik, Metallmansgränden 2–6, PB 1703, 02044 VTT
tel. växel (09) 4561, fax (09) 463 118
VTT Manufacturing Technology, Materials Technology, Metallimiehenkuja 2–6, P.O.Box 1703,
FIN–02044 VTT, Finland
phone internat. + 358 9 4561, fax + 358 9 463 118

VTT Valmistustekniikka, Käyttötekniikka, Kemistintie 3, PL 1704, 02044 VTT
puh. vaihde (09) 4561, faksi (09) 456 7002
VTT Tillverkningsteknik, Driftsäkerhetsteknik, Kemistvägen 3, PB 1704, 02044 VTT
tel. växel (09) 4561, fax (09) 456 7002
VTT Manufacturing Technology, Operational Reliability, Kemistintie 3, P.O.Box 1704,
FIN–02044 VTT, Finland
phone internat. + 358 9 4561, fax + 358 9 456 7002

VTT OFFSETPAINO, ESPOO 1996

Salonen, Jorma & Auerkari, Pertti. Microstructural degradation in compound tubes. Espoo 1996, Technical Research Centre of Finland, VTT Publications 279. 18 p. + app. 11 p.

UCD 621.643:620.1:620.187
Keywords microstructure, degradation, thermal degradation, tubes, temperature, materials, hardness, measurement, microscopes, carbides, carburizing

ABSTRACT

In order to quantify microstructural degradation at high temperatures, samples of SA 210 / AISI 304 L compound tube material were annealed in the temperature range 540 - 720°C for 1 to 1 000 hours. The hardness of the annealed material was measured and the microstructure of the samples was investigated with optical and scanning electron microscopy. Microstructural degradation was characterised by the carbide structure in the ferritic-pearlitic base material and by the depth of decarburised and carburised zones of the compound tube interface. The observed changes were quantified in terms of their time and temperature dependence and diffusion coefficients of the process. The results can be used in estimating the extent of thermal exposure of high-temperature components after long-term service or after incidences of overheating.

PREFACE

This work was performed at VTT Manufacturing Technology and was financially supported by an internal R&D project.

CONTENTS

1 INTRODUCTION

To assess the service condition and useful life of high temperature components such as boiler tubes, it is essential to evaluate the effects of the thermal service history. However, since direct long-term monitoring of the material temperatures from boiler tubes is not easy, the thermal service history is more conveniently assessed from the material-specific thermal changes of the microstructure by metallographic evaluation of boiler tube samples.

In unalloyed and low alloyed steels with ferritic-pearlitic initial microstructure, in-service changes start as disintegration and gradual spherodisation of the pearlite lamellae, followed by coarsening of the carbides and gradual disappearance of the original pearlitic (eutectoidic) regions (Toft & Marsden 1961; Viswanathan 1989). The changes can be observed microscopically from polished and etched metallographic specimens. Because the microstructure correlates with mechanical properties, these properties (eg. hardness) can also show the corresponding change in the microstructure.

To improve resistance to external high temperature corrosion, the so-called compound (or composite) tubes feature a layer of austenitic stainless steel (or other high-alloy material) on top of a carbon steel tube. In such tubes the microstructural changes in service are not limited to the usual changes in the base materials, but in addition changes will occur on the interface between the unalloyed and high-alloyed steels. In particular, carbon is expected to diffuse from the unalloyed to the austenitic steel and hence to exhibit simultaneous decarburisation on the unalloyed side and carburisation and sensitisation on the austenitic side.

The thermal degradation of the carbide structure of a ferritic-pearlitic steel can be expected to follow general Arrhenius type kinetics with a reaction rate of

$$dV/dt = Ae^{-Q/kT}, \quad (1)$$

where A is a material dependent constant, Q is the apparent activation energy of degradation, k is the Boltzmann constant and T is absolute temperature (K).

This means that for an equal state after such a reaction, the time and temperature required for a change by the reaction to this state show linear dependence in $1/T$-log t coordinates. To give a numerical value for such a state, i.e. a combination of time and temperature to yield the same microstructure, Equation 1 can be simplified to a number of parametric expressions, the commonest one being the Larson-Miller parameter

$$P_{LM} = T \times (\log t + C), \quad (2)$$

where *t* is time (h) and C is a material- and reaction-dependent constant. Previous work on the microstructural degradation of boiler steels (Salonen 1994) suggests that generally for these steels C ≈ 14.

The mass transfer of carbon across the interface of a compound tube occurs by diffusion. For steady state diffusion across an approximately planar interface and diffusion distance x

$$x^2 \sim D\,t, \tag{3}$$

where $D = D_o\exp(-Q/kT)$ is the diffusion coefficient which also shows an Arrhenius type temperature dependence according to Equation 1. Therefore, a given change by diffusion can again be expected to lie on a straight line in $1/T$ - log t coordinates.

For Equation 3 to hold true, e.g. for the depth of decarburisation of the carbon steel side in the compound tube, the boundary concentrations should remain stable during annealing. This is unlikely if, for example, the carburisation of the austenitic layer increases the carbon concentration throughout the layer.

2 MATERIALS AND METHODS

2.1 MATERIALS

The selected test materials were delivered as a commercial grade compound tube with the inner part of carbon steel ASME SA 210 (corresponding approximately to St 45.8 DIN 17175) and outer part of austenitic stainless steel AISI 304 L. Table 1 shows the chemical composition according to the manufacturers' certificates and the corresponding standard requirements. Table 2 shows the mechanical properties of the test materials. Steel SA 210 is compared here with St 45.8 DIN 17175.

Table 1. Chemical composition of the materials (wt-%).

Steel		**C**	**Si**	**Mn**	**Cr**	**Ni**
SA 210	1)	0.20	0.26	0.71		
St 45.8	2)	≤ 0.21	0.10-0.35	0.40-1.20		
AISI 304 L	1)	0.016	0.39	1.28	18.3	10.1
	2)	≤ 0.03	≤ 1.0	≤ 2.0	18 - 20	8 - 12

1) According to manufacturer's certificate
2) Required for St 45.8 by DIN17175 and for SA210/304L by ASME.

Table 2. Mechanical properties of the materials at room temperature.

Steel type	Dimensions mm	Rm N/mm^2	ReL N/mm^2	A5 %
SA 210 1)	ø 60.2 x 4.9	510	316	31
St 45.8 2)		410 - 530	≥ 255	≥21
AISI 304 L 2)	ø 63.5 x 1.65	≥480	≥170	≥30

1) According to manufacturer's certificate
2) For St 45.8 acc. to DIN 17 175, for 304 L acc. to ASME.

Carbon steels like SA 210 are delivered in a normalised state, and for welded products a post-weld heat treatment (PWHT) is possible but often not required for boiler tubes. The heat treatment characteristics of the steels are shown in Table 3.

Table 3. Heat treatment characteristics of the ferritic test materials.

Steel	A1	Normalising	PWHT
SA 210 / St45.8	~ 725°C	870 - 900°C 1)	520 - 600°C
Compound tube	-	920°C 2)	-

1) According to DIN 17175 for St 45.8
2) Normalising/solution anneal temperature of compound tube according to manufacturer's certificate.

2.2 METHODS

Samples taken from the compound tube material were annealed isothermally using temperatures of 540, 600, 660 and 720°C and a range of annealing times from 1 to 1 000 hours. The annealing time ranges for each temperature are shown in Table 4.

Table 4. Time and temperature combinations used in annealing tests.

Material	Annealing temperature (°C)	Annealing times (h)
Compound tube	540	10 - 300
”	600	1 - 1 000
”	660	1 - 300
”	720	1 - 100

Light optical microscopy (LOM) was used to inspect the microstructure of the annealed base material samples. Selected samples of these were further investigated using scanning electron microscopy (SEM).

In addition, decarburisation of the unalloyed steel and carburisation and sensitisation of the austenitic steel were investigated with LOM from the interface region of the compound tube samples. Hardness (HV5) was measured from the base materials according to SFS 3214.

3 RESULTS AND DISCUSSION

3.1 MICROSTRUCTURAL CHANGES

The microstructural changes observed after isothermal annealing are shown for the SA 210 base material in the seven example micrographs of Appendix 1 (LOM) and in the 10 example micrographs of Appendix 2 (SEM).

The microstructural changes were classified according to the following scale (for ferritic-pearlitic steels):

A	Microstructure of new steel, ferrite + pearlite
B	First indications of disintegration of the pearlite lamellae
C	Considerable spherodisation, still some lamellar carbides
D	No lamellar carbides, but pearlitic carbides remain mainly in eutectoid grains
E	Carbides widely spread, some eutectoid grains still discernible
F	Original pearlitic regions no longer visible, some carbides very coarse
G	As F but showing also ferrite grain growth.

The microstructural changes in steel SA 210 are shown in Figure 1 in $1/T$ - log t coordinates. Classification is based on LOM examination only.

It is seen that to achieve an equal state of microstructural degradation, the time-temperature combinations lie on straight lines corresponding to a Larson-Miller-parameter constant of C ≈ 14. In addition to carbide changes, graphitisation was observed in steel SA 210 at 720°C after more than 30 h annealing.

3.2 HARDNESS

The measured hardness in steel SA 210 is shown in Figure 2. It is seen that thermal exposure leading to equal hardness lies approximately on straight lines with similar slopes to the correponding lines for microstructural changes (Figure 1).

The limits of the room temperature minimum tensile strength of DIN 17175, based on measured hardness, are also shown in Figure 2.

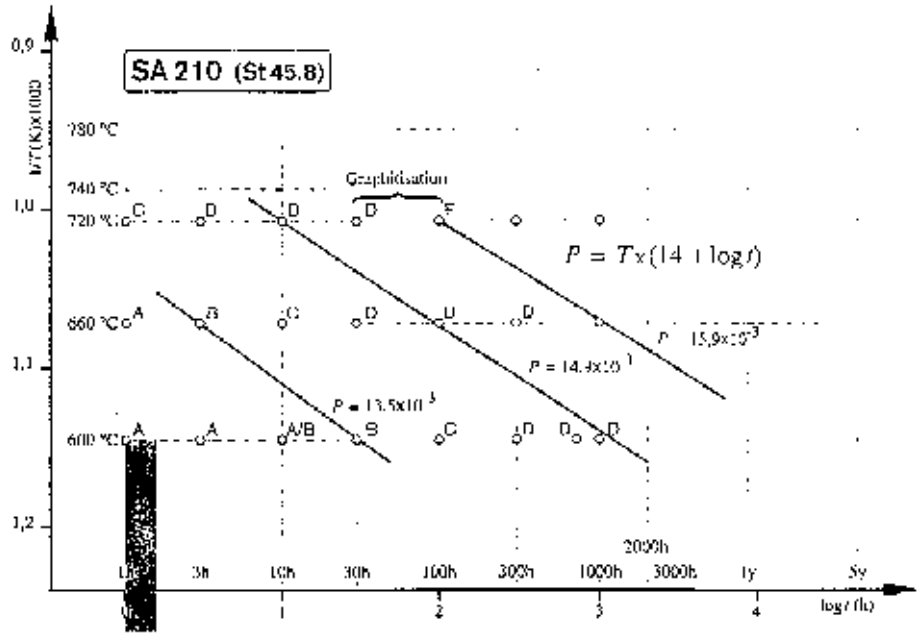

Fig. 1. Time and temperature dependence of the microstructural evolution in steel SA 210.

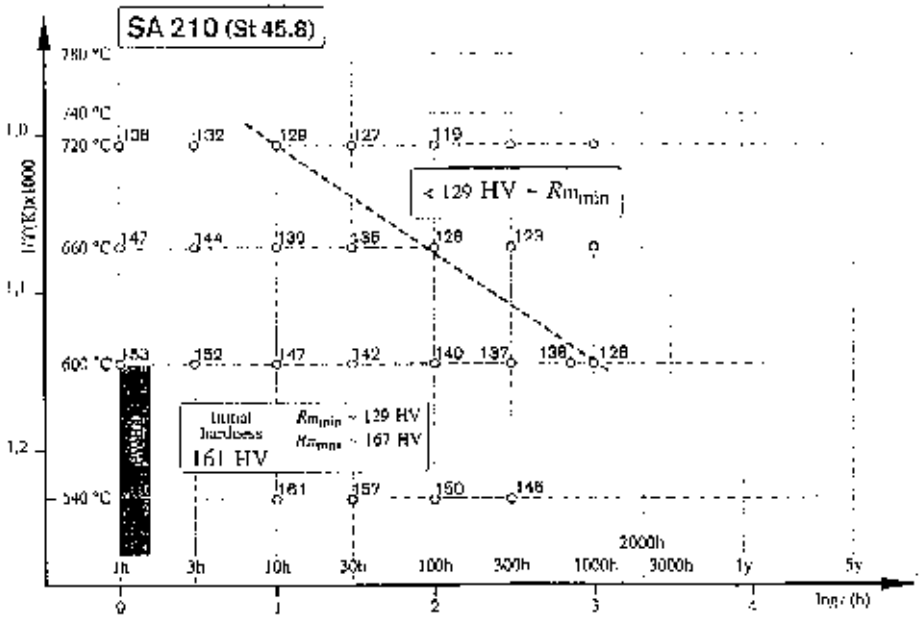

Fig 2. Time and temperature dependence of hardness in steel SA 210.

3.3 DECARBURISATION OF CARBON STEEL ON THE COMPOUND TUBE INTERFACE

Table 5 shows the depth of decarburisation as measured with LOM from the cross-section of annealed compound tube samples. Examples of actual appearance in the corresponding micrographs are shown in Appendix 3. The depth of decarburisation has been measured as the depth of partial decarburisation (total thickness of the layer where some decarburisation is seen in LOM) and as the depth of full decarburisation (thickness of the ferritic layer with no visible pearlite regions). Equation 3 predicts a linear dependence between the depth of decarburisation and the square root of time. However, it is clear that decarburisation has proceeded also during the manufacturing processes of the compound tubes. For this reason the apparent annealing times t_o, corresponding to the depth of decarburisation in the as-new state, have been calculated using Equations 3 and 4. The results are shown in Table 6. Figure 3 shows the testing results corrected by this value of t_o.

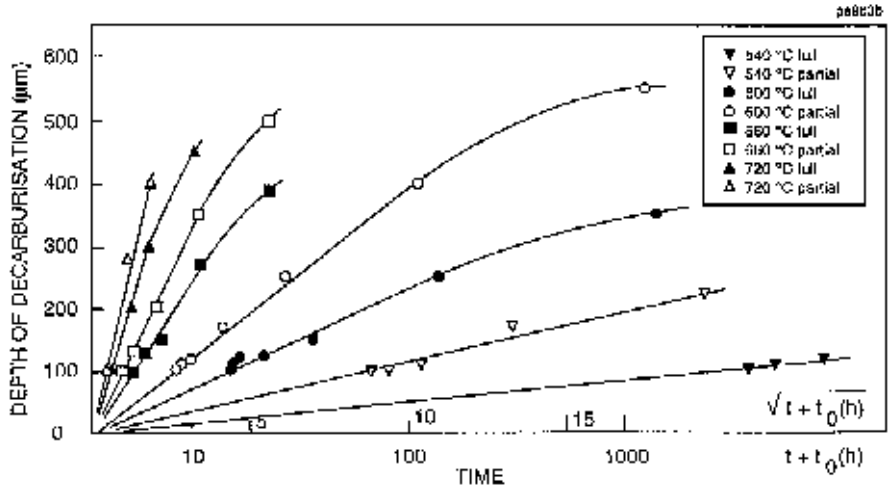

Fig. 3. Depth of decarburisation on the compound tube interface as a function of time, corrected by the time t_o of manufacturing-related initial decarburisation.

Table 5. Depth of decarburisation on the interface of a compound tube (carbon steel side).

Annealing temperature °C	**Annealing time h**	**Depth of full decarburisation µm**	**Depth of partial decarburisation µm**
As new		**100**	**100**
540	10	100	100
	30	110	110
	100	120	170
	300	130	220
600	1	110	110
	3	120	120
	10	120	170
	30	150	250
	100	250	400
	300	350	550
	700	450	850
660	1	130	130
	3	150	200
	10	270	350
	30	380	500
	100	600	850
	300	800	1 200
720	1	200	280
	3	300	400
	10	450	800
	30	700	900

Table 6. Annealing time and temperature combinations corresponding to the decarburisation depth of carbon steel in a new compound tube.

Annealing temperature °C	**Annealing time t_0**	
	Full decarburisation h	**Partial decarburisation h**
540	435	78
600	19	6.7
660	1.6	0.9
720	0.4	0.2

The results corrected by the nominal initial exposure t_o are linear up to a depth of decarburisation of about 200 - 300 µm, beyond which the growth rate of the decarburised layer decreases, possibly due to carburisation of the austenitic steel.

The results are shown in Figures 4 and 5 in $1/T$ - log t coordinates, where time and temperature combinations leading to equal depth of decarburisation appear to lie on the same straight lines, as required by Equation 4. The slopes of these lines appear similar to those in Figure 1 of corresponding microstructural changes in the base material. This suggests that also the depth of decarburisation can be extrapolated to different thermal exposures using the Larson-Miller-parameter $P_{LM} = T \times (14 + \log t)$.

Furthermore, the results show that changes seen under LOM become apparent with less thermal exposure in decarburisation than in the microstructural changes of the base material. This sensitivity suggests that measuring the depth of decarburisation is a particularly useful approach for assessing the thermal history of compound tubes, at least if notable overheating has not occurred.

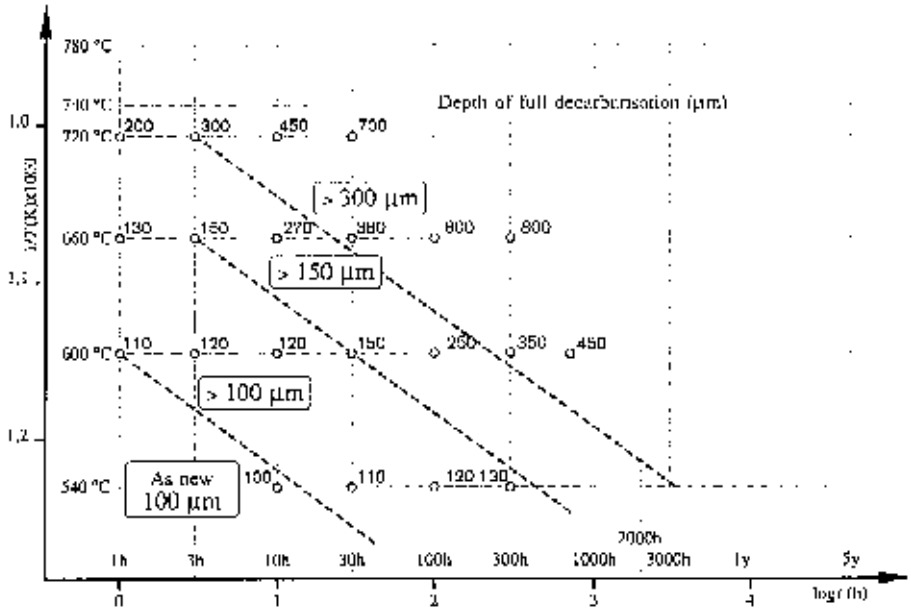

Fig. 4. Time-temperature dependence of the depth of full decarburisation.

For the as-new depth of decarburisation of 100 µm, the combined time-temperature loading of any sample compared with the corresponding isothermal anneal can be estimated from Figures 4 and 5. As measuring the depth of decarburisation is a somewhat subjective matter, more consistent results are likely by using the example micrographs of Appendix 3.

If the as-new depth of decarburisation deviates from 100 µm, the required correction to the initial thermal exposure can be estimated from Figure 3.

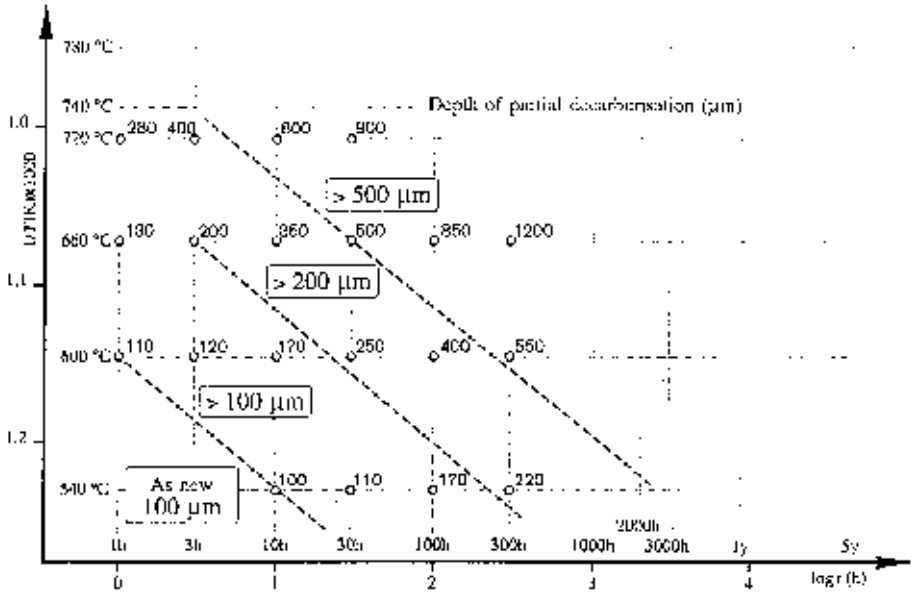

Fig. 5. Time-temperature dependence of the depth of partial decarburisation.

3.4 CARBURISATION OF AUSTENITIC STAINLESS STEEL ON THE BOUNDARY OF A COMPOUND TUBE

Examples of microstructural changes caused by carburisation of the austenitic stainless steel side boundary are shown in Figure 2 of Appendix 3. These samples show carburisation as growth of a sensitised layer etching strongly at grain boundaries and an interface layer (adjacent to the carbon steel) containing carbides also inside the grains. LOM was used to measure the distance from the interface to the outer limit of partial sensitisation (zone where part of the grain boundaries etch strongly) and to the outer limit of full sensitisation (zone where all grain boundaries etch strongly). The results are shown in Table 7 and in Figure 6.

Comparison with the results from decarburisation of the carbon steel side (Table 5 and Figure 3) shows that discernible changes are seen under LOM both in decarburisation of the carbon steel and sensitisation of the austenitic steel after a roughly similar thermal history. However, sensitisation of the austenitic steel proceeds relatively quickly though the whole thickness of the austenitic steel. This suggests that sensitisation takes place partially due to the original carbon in the

austenitic material, and is relatively sensitive to this original carbon content. Less pronounced sensitivity is expected to the carbon content of the carbon steel when measuring depth of the decarburised zone, and this measure therefore appears preferable when estimating the actual thermal service history of ex-service boiler tube samples.

Table 7. Thickness of fully and partially sensitised zones (µm) on the stainless side of a compound tube interface region.

Temperature °C	**Annealing time h**	**Thickness of fully sensitised zone µm**	**Thickness of partially sensitised zone µm**
As new		**100**	**110**
540	10	100	110
	30	140	200
	100	160	230
	300	210	through thickness
600	1	100	120
	3	110	170
	10	170	220
	30	220	350
	100	250	through thickness
	300	350	through thickness
660	1	150	180
	3	160	210
	10	190	230
	30	220	through thickness
	100	350	through thickness
	300	550	through thickness
720	1	170	200
	3	200	230
	10	220	250
	30	320	through thickness
	100	500	through thickness

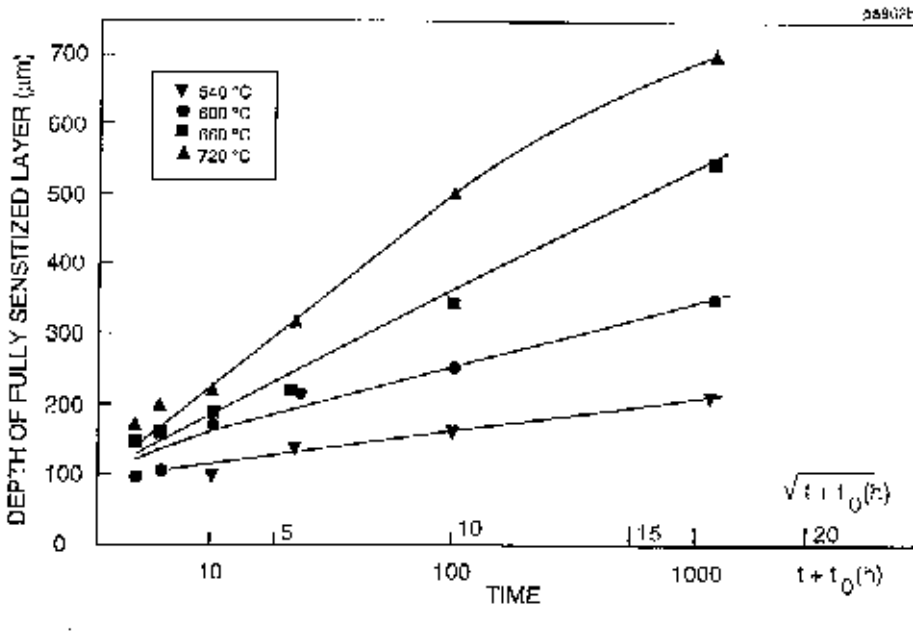

Fig. 6. Thickness of the fully sensitised (all grain boundaries) zone in austenitic steel as measured from the compound tube interface.

3.5 DIFFUSION KINETICS

The overall diffusion coefficients D for the processes of interface decarburisation and austenite sensitisation can be determined from the above time-diffusion distance measurements using Equation 3. The results are shown in Table 8 and Figure 7.

Table 8. Diffusion coefficients corresponding to depth of decarburisation and sensitisation.

Temperature °C	**Full decarburisation lgD(cm^2 /s)**	**Partial decarburisation lgD(cm^2 /s)**	**Full sensitisation lgD(cm^2 /s)**
540	-10.19	-9.45	-9.50
600	-8.84	-8.38	-9.08
660	-7.76	-7.51	-8.57
720	-7.13	-6.86	-8.18

The obtained value of D for sensitisation of the stainless steel appears to agree reasonably well with the diffusion coefficient of carbon in austenite. In contrast, the values of D for decarburisation of the carbon steel do not seem to agree well with the diffusion coefficient either in austenite or ferrite. Therefore the probable rate-determining step in the process of carbon transfer from the unalloyed steel to the stainless steel side is carbon diffusion across the interface to the austenitic base material. This is not unexpected considering the low diffusion coefficient of carbon in austenite.

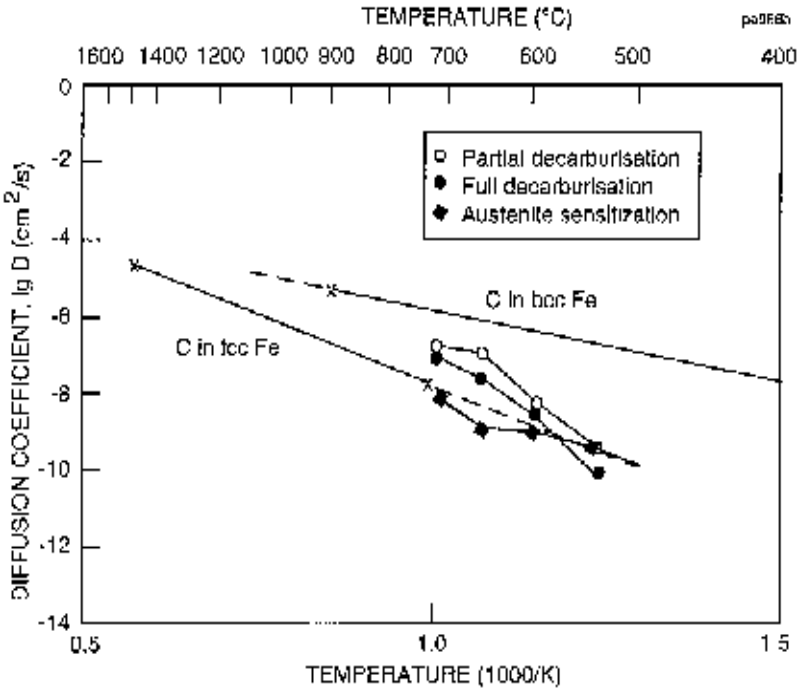

Fig. 7. Diffusion coefficients obtained from measured depth of decarburisation and sensitisation compared with the diffusion coefficients of carbon in bcc and fcc iron from the literature (Metals Handbook 1984).

4 SUMMARY

To evaluate different types of thermal degradation in typical compound tubes used for recovery boilers, samples of a SA 210/AISI 304 L compound tube material were annealed in the temperature range 540 - 720°C for 1 to 1 000 hours. The hardness of the annealed material was measured and the microstructure of the samples was investigated with optical and scanning electron microscopy. Microstructural degradation was evaluated as carbide structure in the ferritic-pearlitic base material, and as depth of decarburisation and carburisation on the compound tube interface. The observed changes were quantified in terms of their time-temperature dependence and diffusion coefficients of the rate-determining process. The results can be used in determining the thermal history of compound boiler tubes after long-term service or overheating excursions.

REFERENCES

Metals Handbook, 1984. Desk Edition. Metals Park, Ohio, USA: ASM. Pp. 28 - 44.

Salonen, J. 1994. Microstructural changes of high temperature steels during long term annealing. Espoo: Technical Research Centre of Finland. 28 p. + app. 40 p. (VTT Julkaisuja - Publikationer 789, in Finnish).

Toft, L. H. & Marsden, R. A. 1961. The structure and properties of 1% Cr-0.5% Mo steel after service in CEGB power stations. Structural processes in creep. London: ISI. Pp. 276 - 294 (ISI Spec. Rep. No. 70).

Viswanathan, R. 1989. Damage mechanisms and the life assessment of high-temperature components. USA. Pp. 183 - 263.

EXAMPLE OPTICAL MICROGRAPHS OF ISOTHERMALLY ANNEALED SA 210

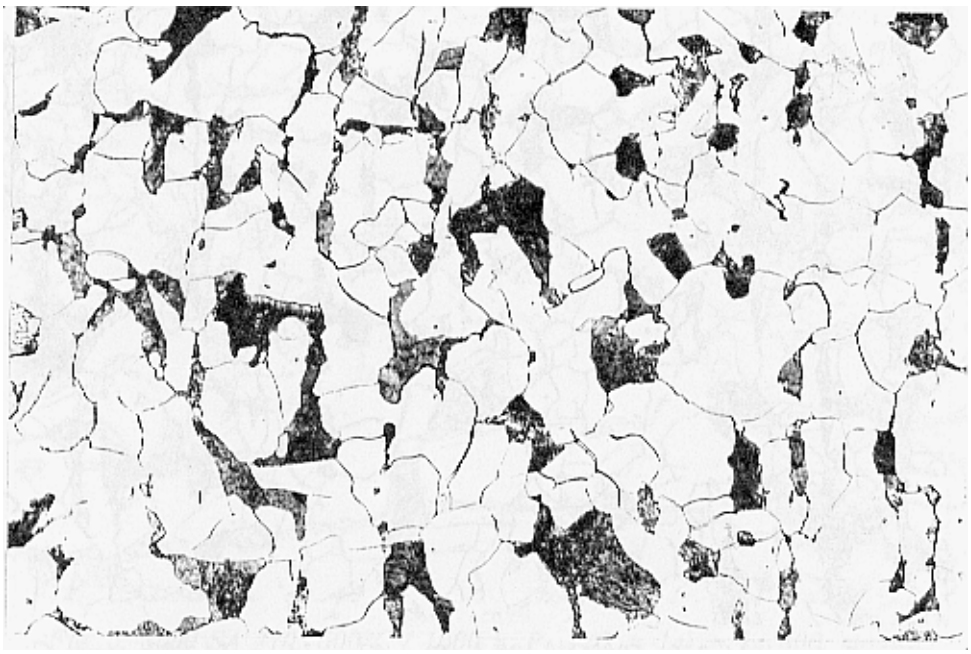

Fig. 1. Steel SA 210: as new, stage A. Magnification 500x.

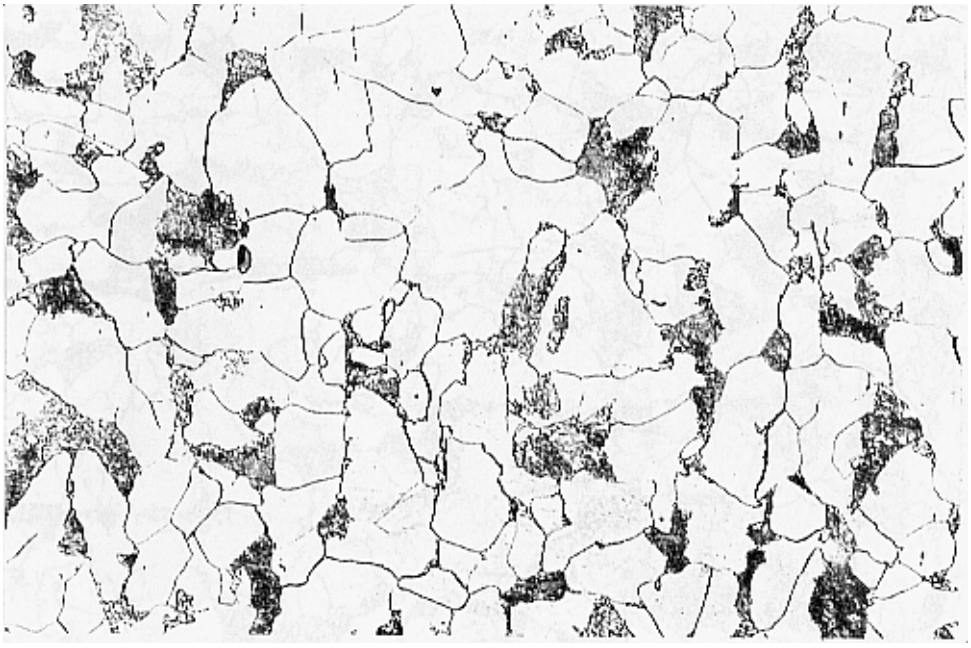

Fig. 2. Steel SA 210: 600°C / 30 h, P_{LM} (C = 14) = 13 500, stage B. Magnification 500x.

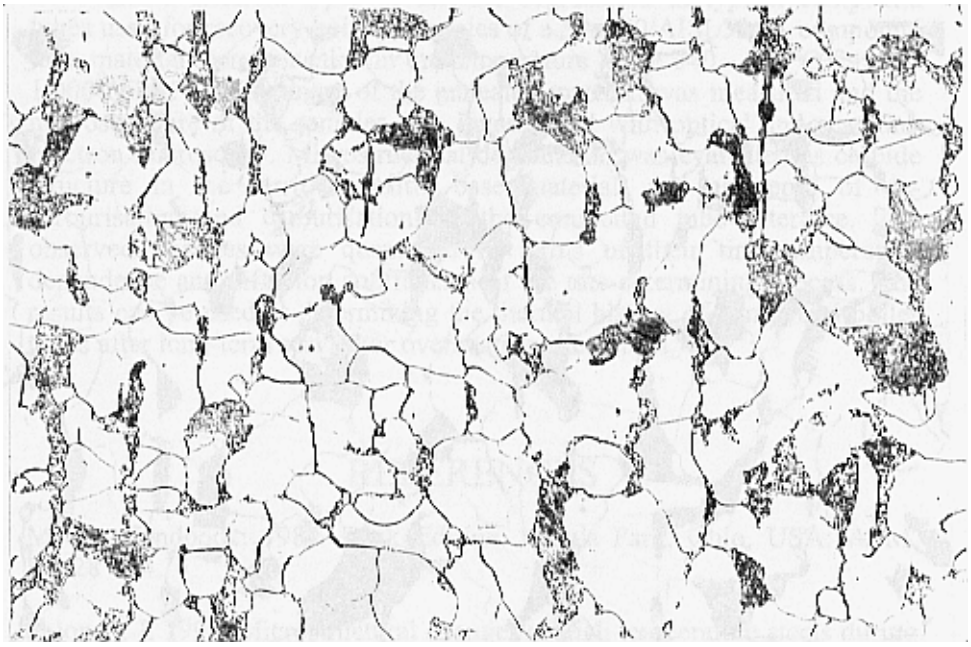

Fig. 3. Steel SA 210: 600°C / 100 h, P_{LM} (C = 14) = 14 000, stage C. Magnification 500x.

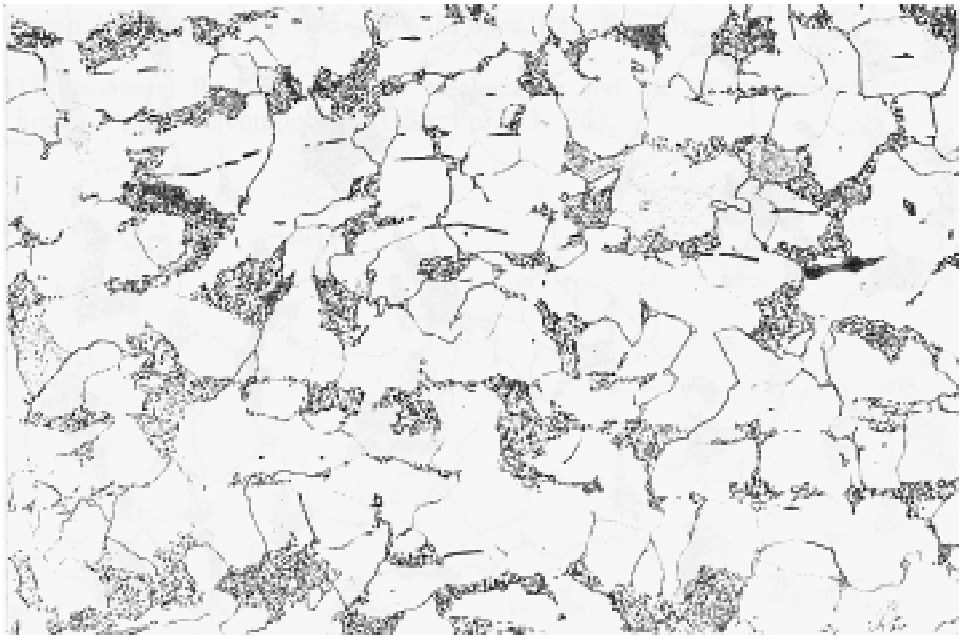

Fig. 4. Steel SA 210: 600°C / 300 h, P_{LM} (C = 14) = 14 400, stage D. Magnification 500x.

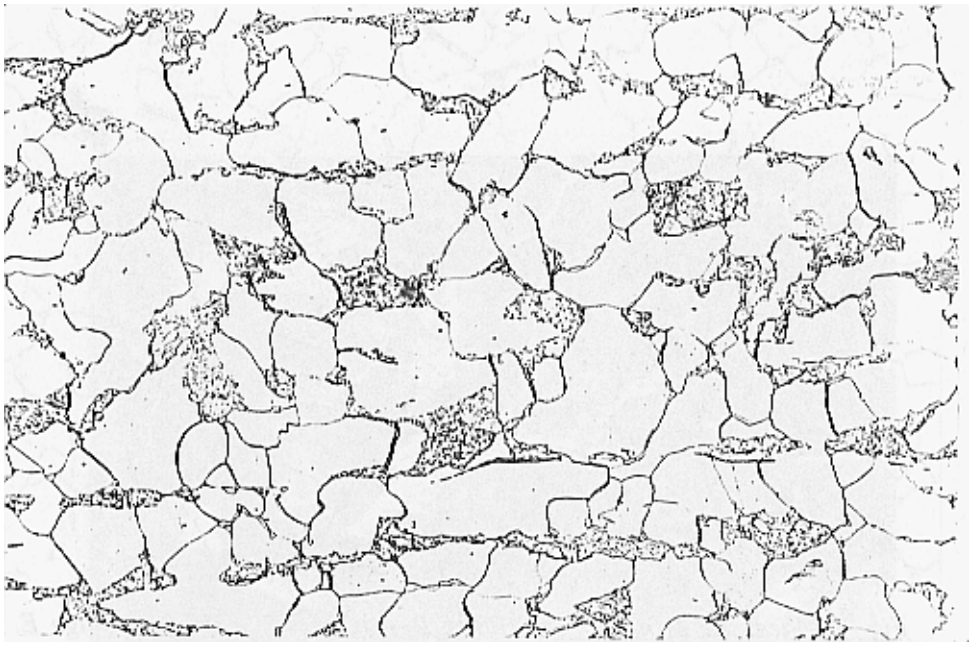

Fig. 5. Steel SA 210: 600°C / 1000 h, P_{LM} (C = 14) = 14 800, stage D. Magnification 500x.

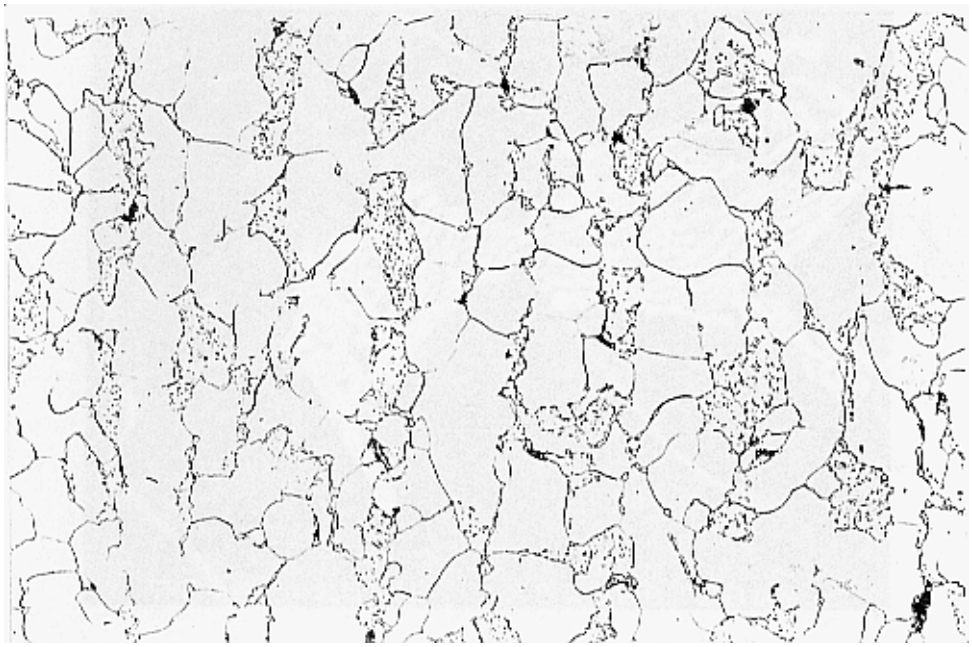

Fig. 6. Steel SA 210: 720°C / 30 h, P_{LM} (C = 14) = 15 400, stage D. Magnifcation 500x.

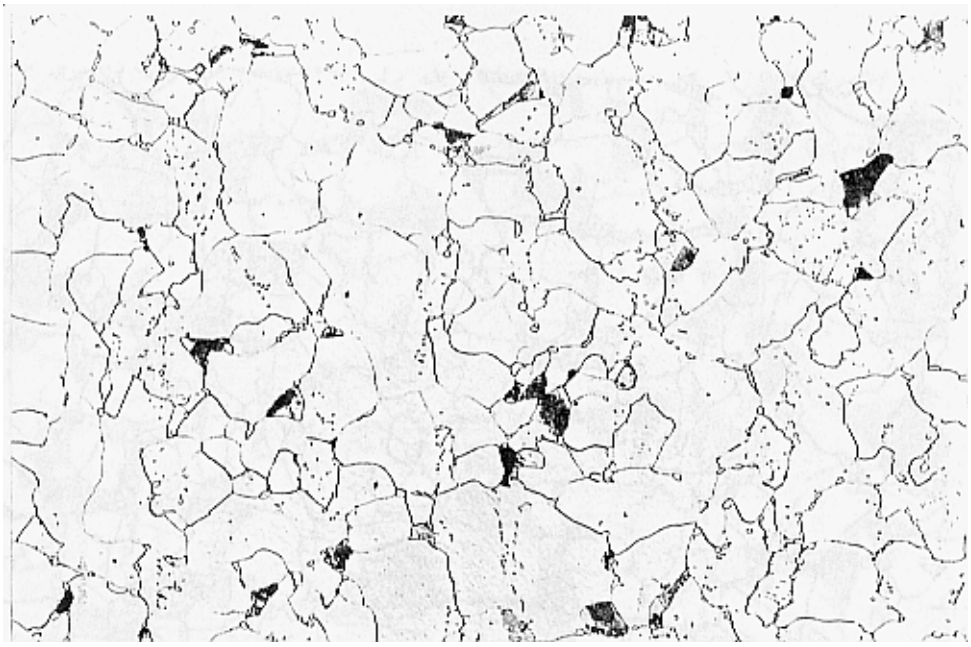

Fig. 7. Steel SA 210: 720°C / 100 h, P_{LM} (C = 14) = 15 900, stage E. Magnification 500x.

SCANNING ELECTRON MICROGRAPHS OF ISOTHERMALLY ANNEALED SA 210

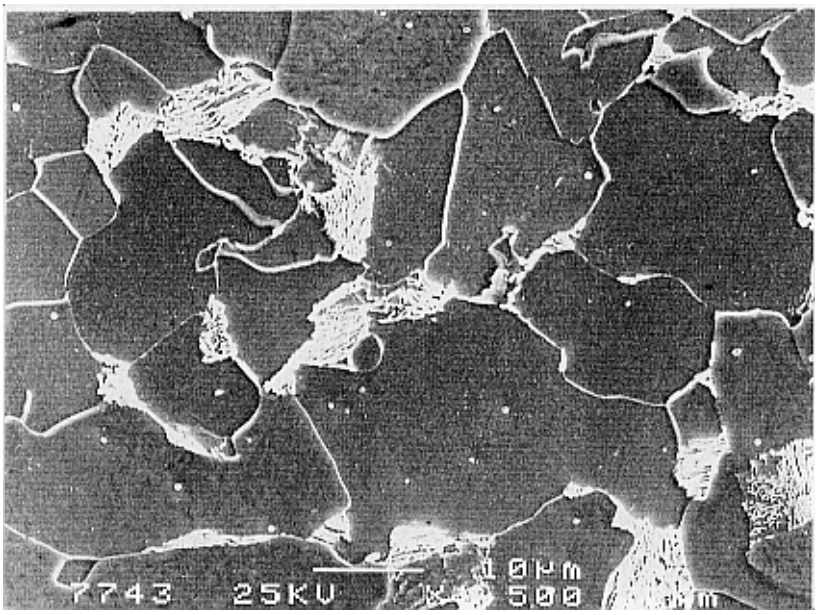

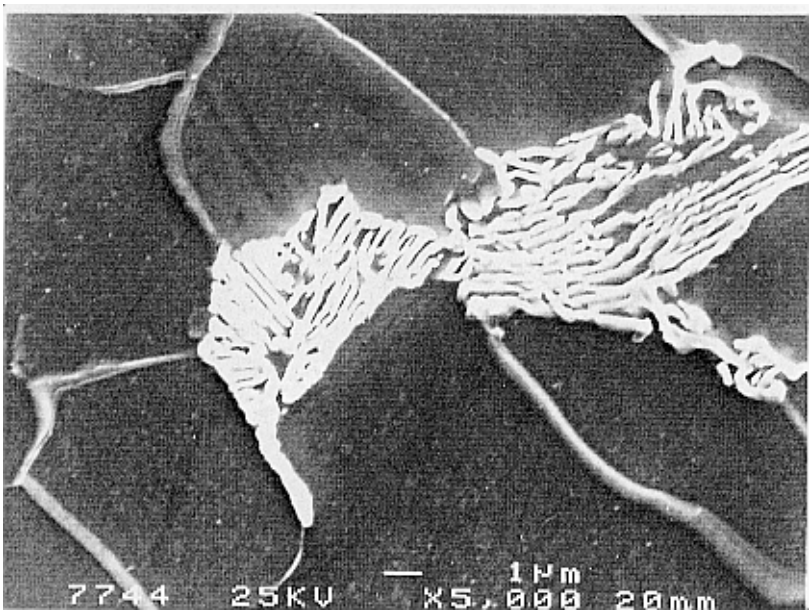

Figs 1 and 2. Steel SA 210: as new, stage A. Magnification 1500x (Fig. 1) and 5000x (Fig. 2).

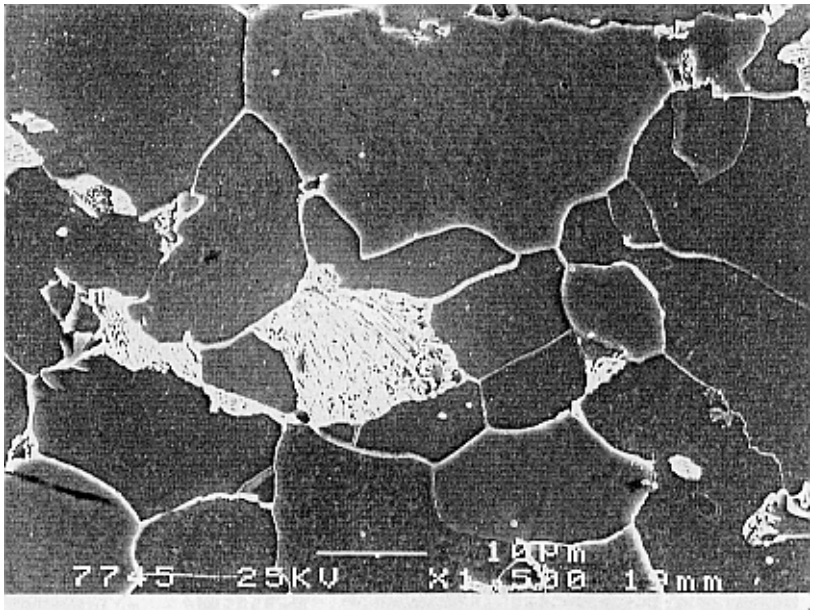

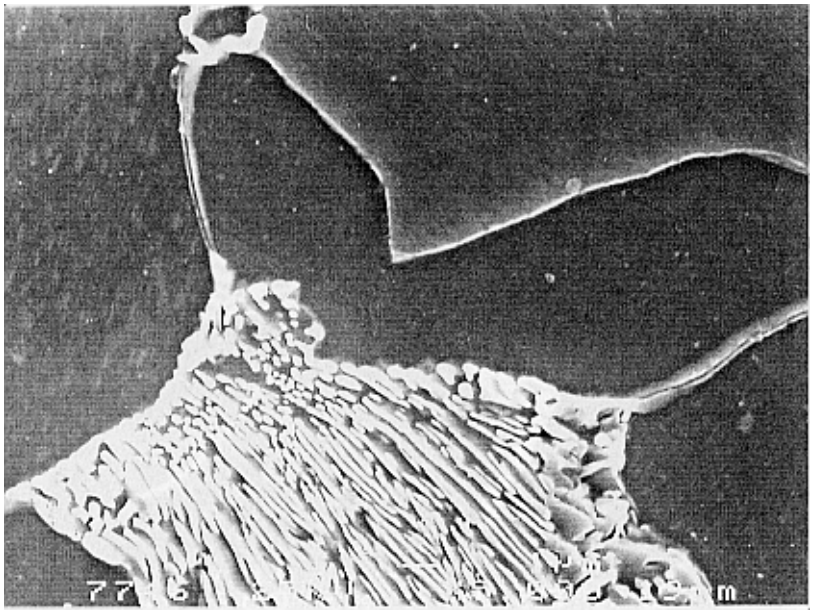

Figs 3 and 4. Steel SA 210: 600°C / 10 h, P_{LM} (C = 14) = 13 100, stage A/B. Magnification 1500x (Fig. 3) and 5000x (Fig. 4).

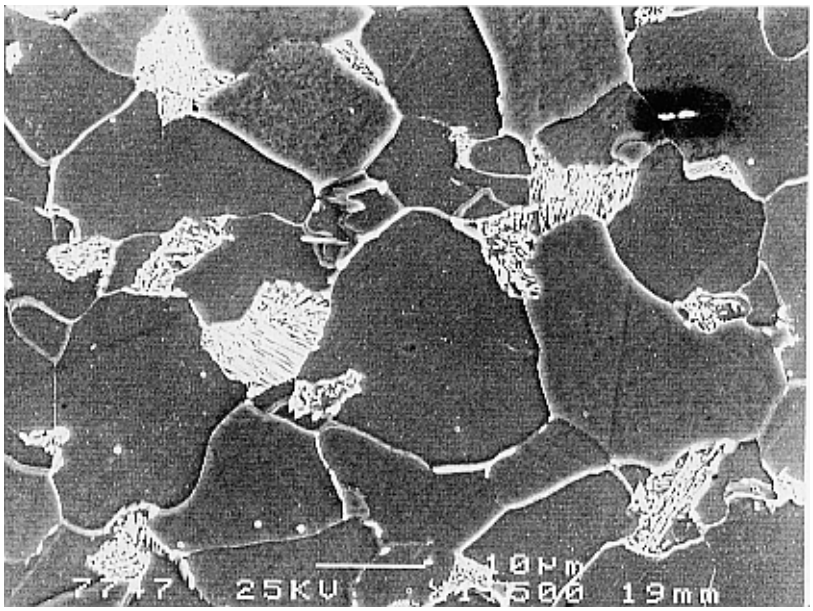

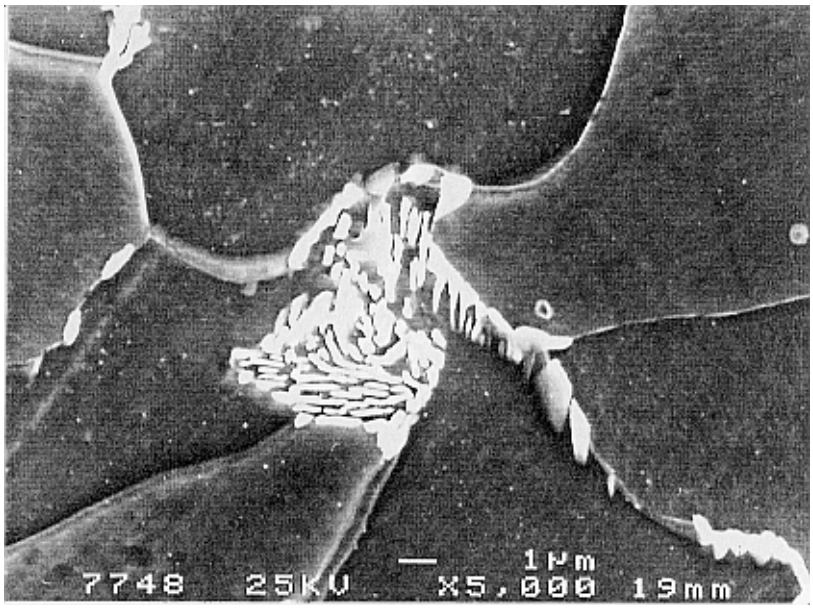

Figs 5 and 6. Steel SA 210: 600°C / 30 h, P_{LM} (C = 14) = 13 500, stage B. Magnification 1500x (Fig. 5) and 5000x (Fig. 6).

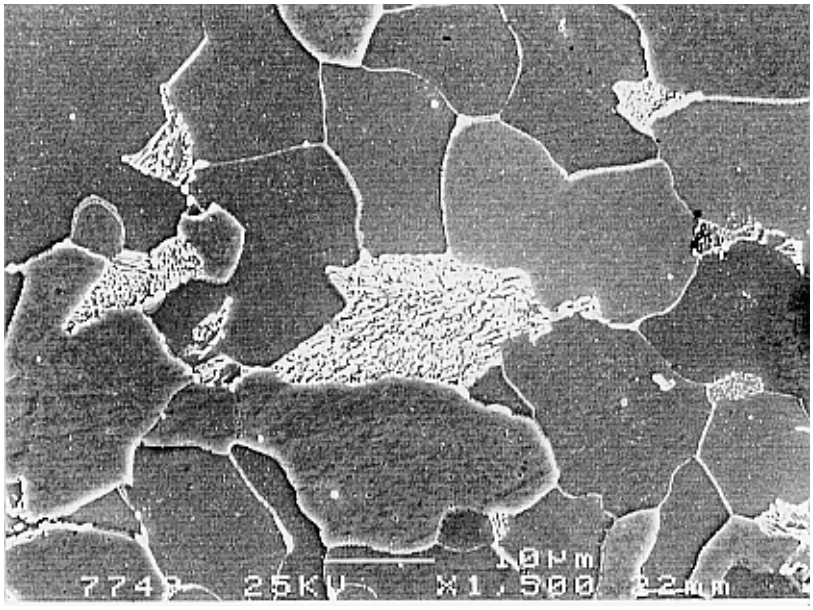

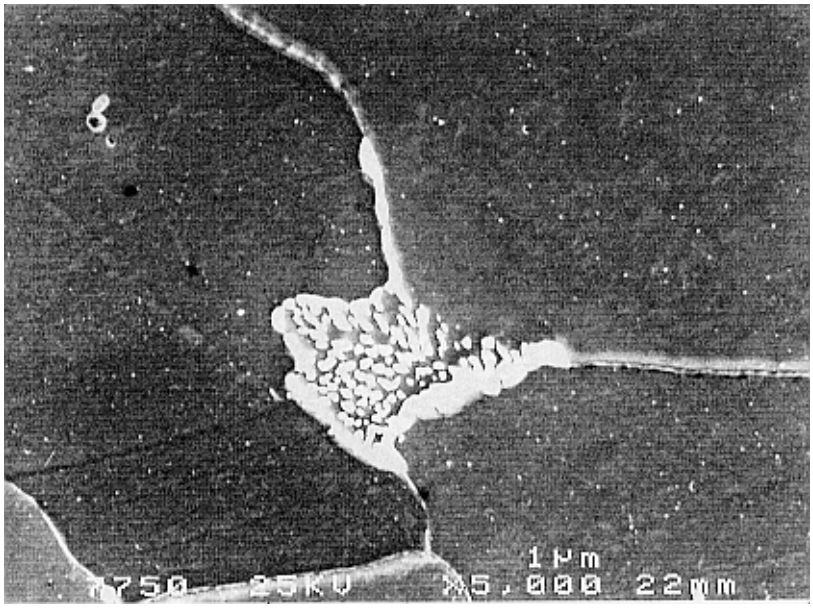

Figs 7 and 8. Steel SA 210: 600°C / 100 h, P_{LM} (C = 14) = 14 000, stage C. Magnification 1500x (Fig. 7) and 5000x (Fig. 8).

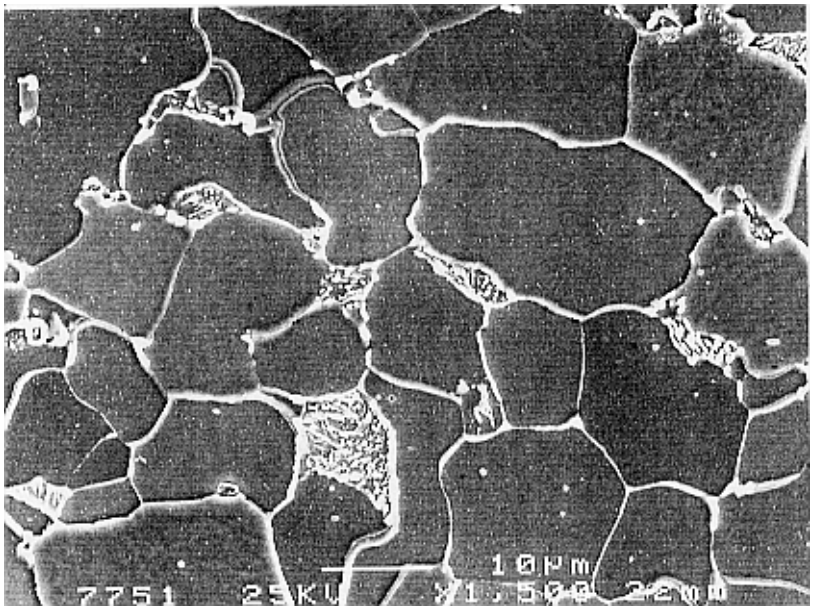

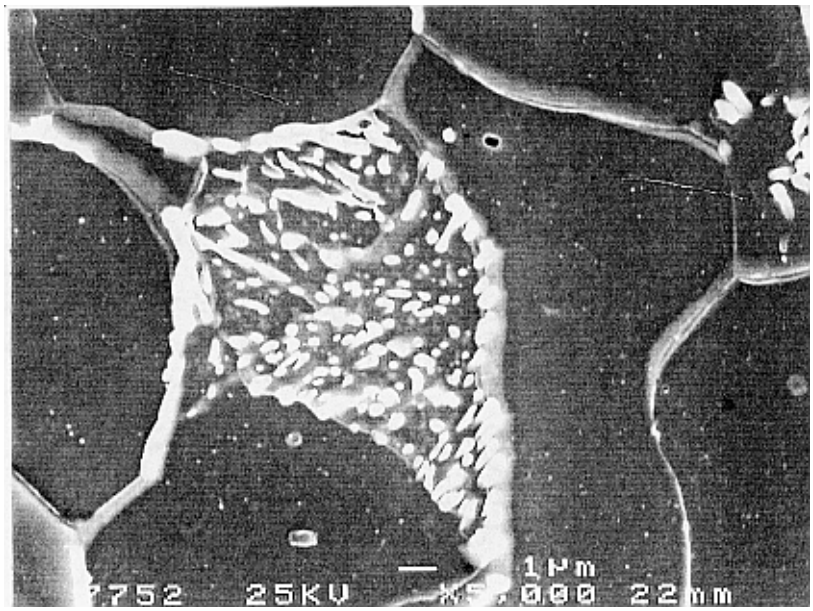

Figs 9 and 10. Steel SA 210: 600°C / 300 h, P_{LM} (C = 14) = 14 400, stage D. Magnification 1500x (Fig. 9) and 5000x (Fig. 10).

DECARBURISATION / CARBURISATION OF THE COMPOUND TUBE INTERFACE

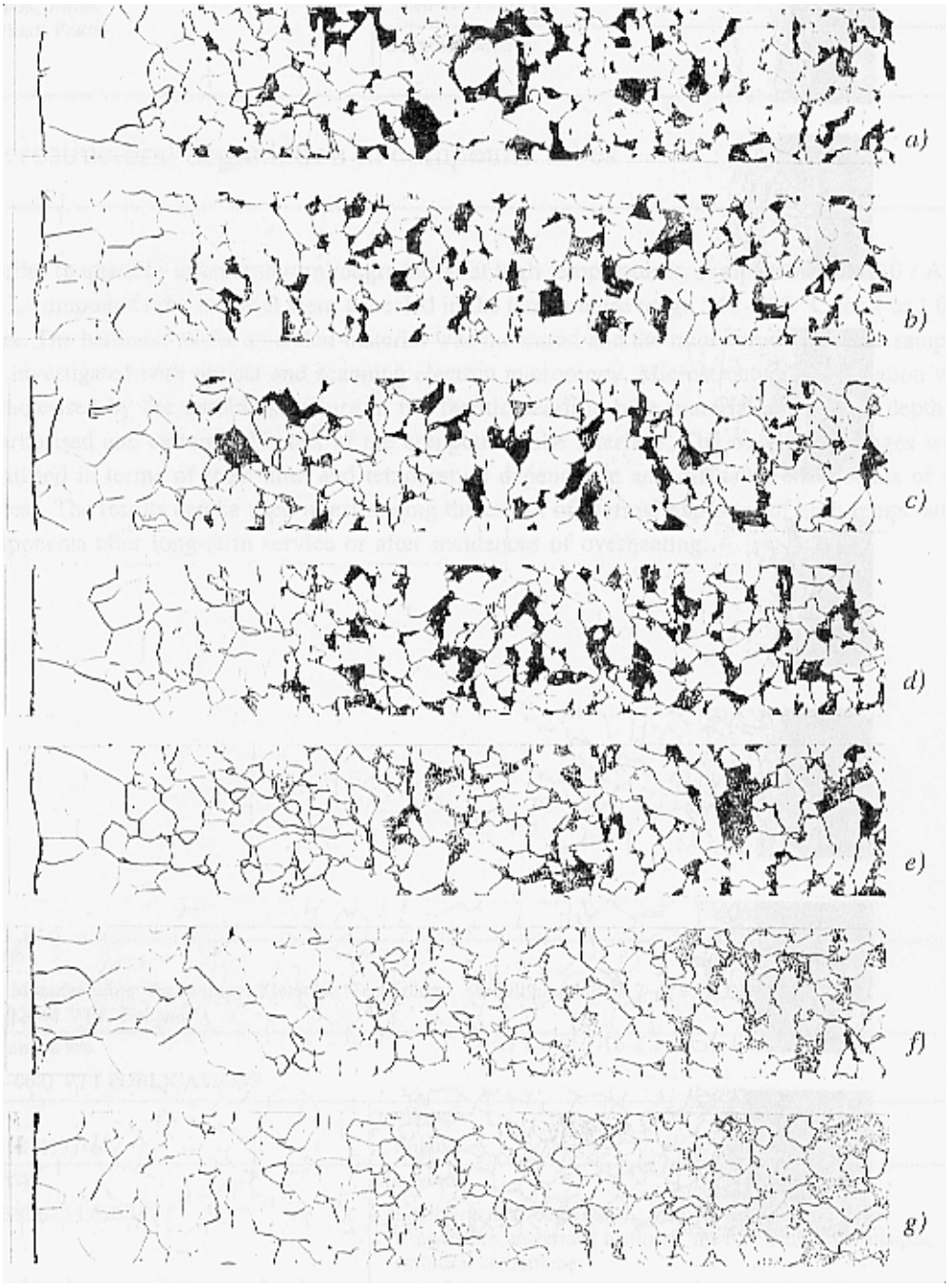

Fig. 1. Interface cross-section of the compound tube, carbon steel side; a) as new; b) 600°C / 1 h; c) 600°C / 3 h; d) 600°C / 10 h; e) 600°C / 30 h; f) 600°C / 100 h and g) 600°C / 300 h. Magnification 200 x.

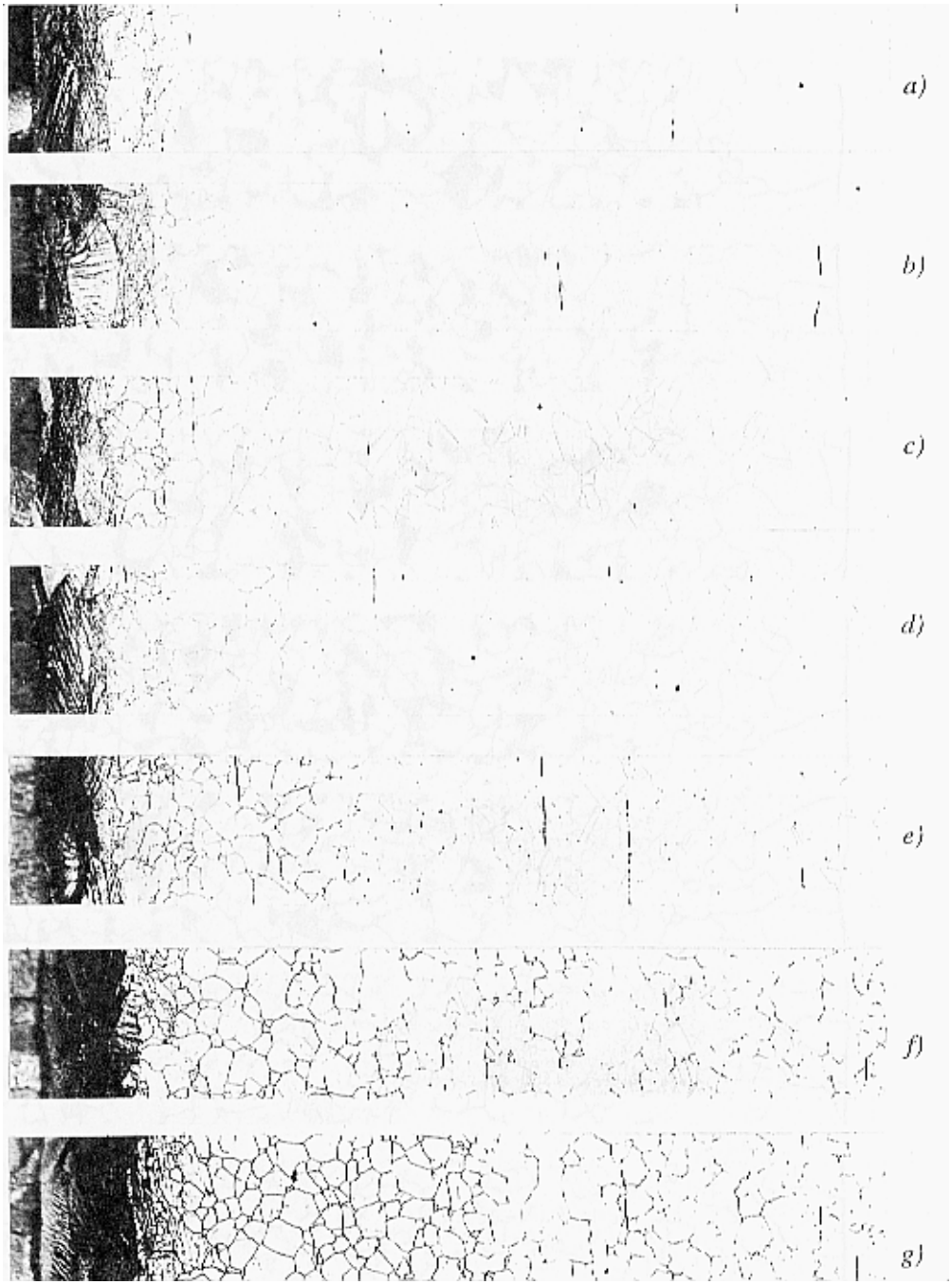

Fig. 2. Interface cross-section of the compound tube, stainless steel side; a) as new; b) 600°C / 1 h; c) 600°C / 3 h; d) 600°C / 10 h; e) 600°C / 30 h; f) 600°C / 100 h and g) 600°C / 300 h. Magnification 200 x.